Immobilization of titanium chiral alkoxides on SBA-15 and modelling the active sites of heterogeneous catalyst using titanium silsesquioxane complexes

Yolanda Pérez, Damián Pérez Quintanilla, Mariano Fajardo, Isabel Sierra*, Isabel del Hierro**

Departamento de Química Inorgánica y Analítica, E.S.C.E.T., Universidad Rey Juan Carlos, 28933 Móstoles, Madrid, Spain

Abstract

A molecular precursor approach involving simple grafting procedures was used to produce site isolated titanium-supported epoxidation catalysts. The complexes $[\{Ti(OiPr)_2(OMent)\}_2]$ (**1**) and $[Ti(OMent)_4]$ (**2**) (MentO = $1R,2S,5R$-(−)-menthoxo) react with the remaining hydroxyl groups of SBA-15 after silanization with Me_3SiCl, via loss of $iPrOH$ and/or menthol and introduction of titanium species onto the silica surface. Grafting **1** and **2** onto SBA-15 yields mostly isolated Ti(IV) sites, as evidenced by DRUV–vis. In addition, the silsesquioxane derivatives $[Ti(OiPr)_2(OMent)\{(c-C_5H_9)_7Si_8O_{13}\}]$ (**3**) and $[Ti(OMent)_3\{(c-C_5H_9)_7Si_8O_{13}\}]$ (**4**) have been synthesized in order to compare the different homogeneous and heterogenous systems mentioned above in the asymmetric epoxidation of cinnamyl alcohol to evaluate their catalytic activity and enantioselectivity.
© 2007 Elsevier B.V. All rights reserved.

Keywords: Silsesquioxane; Mesoporous; Titanium; Alkoxide

1. Introduction

In the current search for heterogeneous catalysts detailed studies of the catalytic activity and recovery experiments have been reported. Numerous synthetic strategies have been described including grafting or tethering of suitable inorganic and organometallic metal precursors by reaction with the silanol groups located on the surface of silica based materials. An increasing number of investigations focus on the development of the supported type metallocene catalyst [1] and heterogeneous constrained-geometry catalysts $[(C_5H_4)SiMe_2(N(CH_2)_3SiMe_2–O–)]M–(NMe_2)_2$ (M = Hf, Zr, Ti) [2] for alkene polymerization and co-polymerization. In addition, there has been considerable attention given to the Ti(IV) silica based materials prepared by reaction of silica or silica ordered mesoporous materials [3] since such surface grafted materials appears to be substantially more active than framework embedded Ti-mesoporous materials in terms

of activity per titanium centre because of the greater accessibility of the grafted metal centres to the reactants. Titanocene Cp_2TiCl_2 [4], titanocenophane $[SiMe_2(\eta^5-C_5H_4)_2]TiCl_2$ [5] and titanium tetraalkoxides [6] have been commonly used as metal precursors, providing effective catalysts for the selective epoxidation of alkenes [7]. Less attention has been paid to the bonding mode of the catalytically active species to the support, although it is clear that for some applications a well define catalyst surface with site-isolated metal centres on the surface is desired, like in the best heterogeneous titanium catalyst where it has been well established that the Ti centres are all four coordinate. In order to approach this problem at molecular level silsesquioxane complexes have been used commonly as model systems for organometallic derivatives supported on silica. Several works have been reported by Duchateau et al. covering this field [8]. The catalytic activity of a number of silsesquioxane titanium alkoxides complexes with mono-, bi- and terdentate ligated silsesquioxanes $R_7Si_7O_9(OH)_3$, $R_7Si_7O_9(OH)_2(OSiR_3)$, $R_7Si_7O_9(OH)(OSiR_3)_2$ (R = c-C_5H_9, c-C_6H_{11}, c-C_7H_{13}, SiR_3 = $SiMe_3$, $SiMePh_2$) has been reported by the groups of Abbenhuis et al. [9], Maschmeyer et al. [10] and Crocker et al. [11]. Titanium derivatives $[TiCp\{(c-C_6H_{11})_7Si_8O_{12}\}]$ and $[TiL\{(c-C_6H_{11})_7Si_7O_{12}\}]$ (L = CH_2Ph,

* Corresponding author.
** Corresponding author. Tel.: +34 914887022; fax: +34 914888143.
E-mail addresses: isabel.sierra@urjc.es (I. Sierra), isabel.hierro@urjc.es (I. del Hierro).
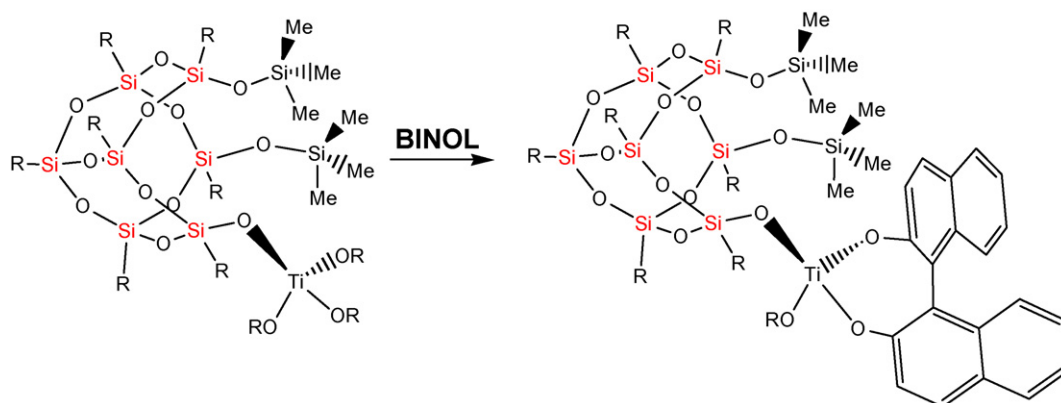
Scheme 1.

NMe$_2$, OSiMe$_3$, Cyclohexyl, OiPr, OMe, OtBu) with a ter-dentate silsesquioxane ligand turned out to be effective and selective epoxidation catalysts producing alkene oxides, as well as Ti(OiPr)$_2$\{(c-C$_6$H$_{11}$)$_7$Si$_7$O$_{11}$(OSiMe$_3$)\}]. The silsesquiox-ane [\{(c-C$_6$H$_{11}$)$_8$Si$_8$O$_{10}$(OH)$_2$\}] with two reactive, isolated, hydroxyl groups easily reacts with TiL$_4$ (L = CH$_2$Ph, Cl) ren-dering titanium containing silsesquioxane gels that catalyse the epoxidation of alkenes, but it is the rapid degeneration of the material through the hydrolysis of the siloxy unit Ti–O–Si that gives the soluble non-siloxy titanium species, Bu^{t}OO-TiL$_3$, active in the process. In comparison titanium complexes with terdentate silsesquioxane ligands provide excellent results in the same experimental conditions, in this case the catalysis occurs through titanium–siloxy complexes. Abbenhuis et al. after their first communication on the titanium silsesquioxanes epoxi-dation catalyst [TiCp\{(c-C$_6$H$_{11}$)$_7$Si$_8$O$_{12}$\}] [12] reported the heterogenization version by the strong adsorption of [TiCp\{(c-C$_6$H$_{11}$)$_7$Si$_7$O$_{12}$\}] on MCM-41 channel molecular sieve. There are few reports on the assemblies of chiral titanium com-plexes over silica-based materials. Johnson and co-workers [13] have published a variety of Ti(IV) complexes in which the titanium is coordinated to only one or two siloxides of the partially silylated silsesquioxane backbone in order to mod-ify the degree of steric congestion around the titanium(IV) active site. This new complexes are performed in their chi-ral version by reaction with the well-known BINOL but they result inactive epoxidation catalysts. Related titanosilsesquiox-ane complexes that do not incorporate these trimethylsilyl groups on the silsesquioxane backbone show significantly higher activity, both in terms of conversion and selectivity (Scheme 1).

Basset and co-workers [14] have reported silica-supported tantalum catalysts for the enantioselective epoxidation of allylic alcohols in the presence of chiral tartrate derivatives with com-parable results to that obtained in the homogeneous sharpless reaction, nevertheless the tantalum precursors are not easy to prepare. A different strategy has been followed by Li and co-workers [15] grafting a chiral tartaric acid onto the surface of silica and in the mesoporous of MCM-41 providing and effective heterogeneous catalyst for asymmetric epoxidation by reaction with Ti(OiPr)$_4$. In a similar way, Seebach and co-workers [16]

has achieved the immobilization of TADDOL onto silica to be used as heterogeneous chiral auxiliar system.

The present study has been carried out in order to see if chiral organometallic fragments can be grafted on surfaces. The main objective in this study is to obtain well-defined organotitanium compounds grafted on silica-based materials in which the chiral moiety is kept bonded to titanium. In a parallel way we have syn-thesized titanium silsesquioxane complexes with a well-defined coordination sphere that may serve as model for the heteroge-neous solids. We wanted to see if the presence of chiral ligands in the coordination sphere of titanium centre makes possible the epoxidation reaction of cinnamyl alcohol.

2. Experimental procedure

2.1. General remarks

All reactions were performed using standard Schlenk tube and dry box techniques under an atmosphere of dry nitrogen or argon. Solvents were distilled from appropri-ate drying agents and degassed before used. Poly(ethylene glycol)-block-poly(propylene glycol)-block-polyethylene gly-col and tetraethoxysilane (TEOS) were purchased from Fluka. Trimethylchlorosilane (Me$_3$SiCl), 3,5,7,9,11,13,15-heptacyclopentylpentacyclo [9.51.1^{3,9}.1^{5,15}.1^{7,13}]octasiloxan-1-ol and (1R,2S,5R)-(−)-menthol were purchased from Aldrich and used as received. Ti(OiPr)$_4$ and NEt$_3$ were distilled and stored under an argon atmosphere prior to use.

2.2. Synthesis of samples

2.2.1. Synthesis of [\{Ti(OiPr)$_3$(OMent)\}$_2$] (1)

Ti(OiPr)$_4$ (0.95 mL, 3.19 mmol) was added to a CH$_2$Cl$_2$ solution (25 mL) of (1R,2S,5R)-(−)-menthol (0.5 g, 3.19 mmol). The resulting solution was stirred at room temperature for 4 h. The solvent and the remaining isopropyl alcohol were removed under vacuum. The resulting product was colour-less oil, spectroscopically pure, after being rinsed twice with cold pentane. Yield 0.98 g, 80%. ^{1}H NMR (300 MHz, CDCl$_3$, 25 °C): δ = 0.75 (d, 3H, $^3J_{H,H}$ = 6.9 Hz, CH_3), 0.88 (d, 6H, $^3J_{H,H}$ = 6.6 Hz, CH_3), 0.82–0.95 (m, 2H, C(4)-H), 1.09–1.16

(m, 2H, C(3)-*H*), 1.21 (d, 18H, $^3J_{H,H} = 6.04$ Hz, –OCH(C*H*$_3$)$_2$), 1.26–1.4 (m, 1H, –C*H*), 1.5–1.61 (m, 2H, C(6)-*H*), 2.05 (m, 1H, C(2)-*H*), 2.34 (m, 1H, C(5)-*H*), 3.88 (m, 1H, C(1)-*H*), 4.45 (h, 3H, –OC*H*(CH$_3$)$_2$). ^{13}C{^{1}H} NMR (300 MHz, CDCl$_3$, 25 °C): $\delta = 15.8$ (*C*H$_3$), 21.1 (*C*H$_3$), 22.7 (*C*H$_3$), 22.2 (*C*$_4$), 25.5 (*C*H), 26.5 (–*C*H(CH$_3$)$_2$), 31.6 (*C*$_5$), 34.6 (*C*$_3$), 46.3 (*C*$_6$), 76.2 (*C*$_1$), 84.4 (–*C*H(CH$_3$)$_2$). IR (Nujol-polyethylene, cm^{-1}): 615(br), 725(s), 849(w), 1007(m), 1049(w), 1068(w), 1082(w), 1124(m), 1373(s), 1460(s), 2665(m).

2.2.2. Synthesis of [Ti(OMent)$_4$] (2)

Ti(O*i*Pr)$_4$ (0.9 mL, 3.03 mmol) was added drop wise to a CH$_2$Cl$_2$ (1*R*,2*S*,5*R*)-(−)-menthol solution (25 mL) (1.9 g, 12.15 mmol). The mixture was stirred for 6 h, then the volatiles were removed getting a colourless oil spectroscopically pure after being rinsed twice with cold pentane (1.76 g, 87%). ^{1}H NMR (300 MHz, CDCl$_3$, 25 °C): $\delta = 0.78$ (d, 12H, $^3J_{H,H} = 6.9$ Hz, C*H*$_3$), 0.9 (d, 24H, $^3J_{H,H} = 6.4$ Hz, C*H*$_3$), 0.81–0.93 (m, 8H, C(4)-*H*), 1.10–1.21 (m, 8H, C(3)-*H*), 1.29–1.4 (m, 4H, –C*H*), 1.5–1.63 (m, 8H, C(6)-*H*), 2.09 (m, 4H, C(2)-*H*), 2.35 (m, 4H, C(5)-*H*), 3.87 (m, 4H, C(1)-*H*). ^{13}C{^{1}H} NMR (400 MHz, CDCl$_3$, 25 °C): $\delta = 15.8$ (*C*H$_3$), 21.2 (*C*H$_3$), 22.3 (*C*H$_3$), 22.7 (*C*$_3$), 25.5 (*C*H), 31.7 (*C*$_5$), 34.6 (*C*$_4$), 46.5 (*C*$_6$), 51.0 (*C*$_2$), 84.1 (*C*$_1$). IR (Nujol-polyethylene, cm^{-1}): 725(s), 849(w), 928(w), 1045(m), 1049(m), 1065(m), 1080(m), 1105(m), 1304(w), 1373(s), 1460(s), 2360(w), 2665(m). TiC$_{40}$H$_{76}$O$_4$ Calc: C 71.82, H 11.45. Found: C 71.06, H 11.32%.

2.2.3. Synthesis of [Ti(OiPr)$_2$(OMent)(c-C$_5$H$_9$)$_7$Si$_8$O$_{13}$] (3)

To a solution of 3,5,7,9,11,13,15-heptacyclopentylpentacyclo[9.51.1^{3,9}.1^{5,15}.1^{7,13}] octasiloxan-1-ol (0.45 g, 0.50 mmol) in THF (30 mL) was added a solution of complex **1** (0.38 g, 0.50 mmol) in THF (10 mL). The resulting solution was stirred for 24 h at room temperature and the solvent removed under vacuum to obtain a white solid. Recrystallization from CH$_2$Cl$_2$ at −30 °C gave **3** as a white crystalline solid. ^{1}H NMR (400 MHz, CDCl$_3$, 25 °C): $\delta = 0.78$ (d, 3H, $^3J_{H,H} = 6.9$ Hz, C*H*$_3$), 0.87 (d, 6H, $^3J_{H,H} = 6.6$ Hz, C*H*$_3$), 0.95 (m, 7H, C*H*-C$_5$H$_9$), 1.18 (d, 12H, $^3J_{H,H} = 5.9$ Hz, –OCH(C*H*$_3$)$_2$), 1.44 (m, 28H, C*H*$_2$-C$_5$H$_9$), 1.54 (m, 14H, C*H*$_2$-C$_5$H$_9$), 1.70 (m, 14H, C*H*$_2$-C$_5$H$_9$), 2.12 (m, 1H, C(2)-*H*(OMent)), 2.35 (m, 1H, C(5)-*H*(OMent)), 3.95 (m, 1H, C(1)-*H*(OMent)), 4.20 (h, 2H, –OC*H*(CH$_3$)$_2$). ^{13}C{^{1}H} NMR (400 MHz, CDCl$_3$, 25 °C): $\delta = 15.9$ (*C*H$_3$), 21.1 (*C*H$_3$), 22.8 (*C*H$_3$), 26.20 (–OCH(*C*H$_3$)$_2$), 34.6 (*C*$_4$), 31.7 (*C*$_5$), 45.9 (*C*$_6$), 50.9 (*C*$_2$) 85.71 (*C*$_1$), 77.21(–O*C*H(CH$_3$)$_2$), 27.39, 27.12, 27.04, 22.37, 22.30, 22.25 (*C*H$_2$-C$_5$H$_9$). ^{29}Si NMR (79.3 MHz, CDCl$_3$, 25 °C): −65.94; −66.65, −112.20 (3:4:1). Nujol-polyethylene, cm^{-1}: 614(br), 663(m), 792(s), 849(m), 912(m), 1009(m), 1082(vs), 1253(w), 1450(w), 2865(w), 2949(w). TiC$_{51}$H$_{96}$O$_{16}$Si$_8$ Calc: C 49.48, H 7.82. Found: C 48.72, H 7.50%.

2.2.4. Synthesis of [Ti(OMent)$_3$(c-C$_5$H$_9$)$_7$Si$_8$O$_{13}$] (4)

To a solution of 3,5,7,9,11,13,15-heptacyclopentylpentacyclo[9.51.1^{3,9}.1^{5,15}.1^{7,13}] octasiloxan-1-ol (0.1 g, 0.13 mmol) in THF (10 mL) was added a solution of complex **3** (0.09 g, 0.13 mmol) in THF (5 mL). The resulting solution was stirred for 24 h at room temperature and the solvent removed under vacuum to obtain a white solid. Recrystallization from CH$_2$Cl$_2$ at −30 °C gave **4** as a white crystalline solid.

^{1}H NMR (300 MHz, CDCl$_3$, 25 °C): $\delta = 0.80$ (d, 9H, $^3J_{H,H} = 7.05$ Hz, C*H*$_3$), 0.90 (d, 18H, $^3J_{H,H} = 6.5$ Hz, C*H*$_3$), 0.95 (m, 7H, C*H*-C$_5$H$_9$), 1.48 (m, 28H, C*H*$_2$-C$_5$H$_9$), 1.57 (m, 14H, C*H*$_2$-C$_5$H$_9$), 1.73 (m, 14H, C*H*$_2$-C$_5$H$_9$), 2.12 (m, 3H, C(2)-*H*(OMent)), 2.33 (m, 3H, C(5)-*H*(OMent)), 3.92 (m, 3H, C(1)-*H*(OMent)). ^{13}C{^{1}H} NMR (300 MHz, CDCl$_3$, 25 °C): $\delta = 15.9$ (*C*H$_3$), 21.1 (*C*H$_3$), 22.5 (*C*H$_3$), 34.6 (*C*$_4$), 31.7 (*C*$_5$), 45.9 (*C*$_6$), 50.9 (*C*$_2$), 85.7 (*C*$_1$), 27.02, 27.31, 27.45, 22.50, 22.28, 22.21 (*C*H$_2$-C$_5$H$_9$). ^{29}Si NMR (79.3 MHz, CDCl$_3$, 25 °C): −66.37, −66.72, −110.86 (3:4:1). IR KBr, cm^{-1}: 505(s), 723(m), 781(w), 852(w), 919(w), 973(s), 1043(w), 1124(s), 1247(m), 1253(w), 1365(w), 1387(w), 1450(m), 2863(m), 2948(m).

2.2.5. Synthesis of SBA-15

A hexagonal (plane group *p*6*mm*) material (SBA-15) was prepared using a poly(alkaline oxide) triblock copolymer surfactant in an acidic medium, according to the method of Zhao et al. [17]. Poly(ethylene glycol)-block-poly(propylene glycol)-block-polyethylene glycol (4.00 g) was dissolved in water (30.00 g) and 2 M HCl (80.00 g) with stirring at 35 °C. TEOS (8.80 g) was added to the homogeneous solution with stirring at room temperature for 20 h. The resulting solid product was filtered off, washed and air-dried at room temperature. The solid was calcinated in an atmosphere of air from room temperature to 500 °C over 8 h and heated at this temperature for 6 h.

2.2.6. Silanol capping reaction

The SBA-15 was dehydrated at 160 °C in vacuo for 5 h and thereafter handled under a nitrogen atmosphere. Typically, a 2 g sample of SBA-15 was suspended in 30 mL of dry toluene and 10 mL (78.79 mmol) of Me$_3$SiCl and triethylamine (78.79 mmol) were added by syringe. The mixture was stirred for 24 h at room temperature and the resulting product SBA-15-SiMe$_3$ was filtered off and washed with toluene (2× 50 mL) and THF (2× 50 mL). The solid material was dried 5 h under vacuum and stored under inert atmosphere.

2.2.7. Immobilization of 1 and 2 on SBA-15-SiMe$_3$ surface

The typical procedure for the preparation of solids Ti1-SBA-15-SiMe$_3$ and Ti2-SBA-15-SiMe$_3$ by reaction of protected SBA-15-SiMe$_3$ and complexes [{Ti(O*i*Pr)$_3$(OMent)}$_2$] (**1**) and [Ti(OMent)$_4$] (**2**), respectively, was as follows. SBA-15-SiMe$_3$ (2 g) was suspended in dry toluene, and to the suspension, stirred mechanically, was added a toluene solution of **1** or **2** (≈5 mmol). The mixture was refluxed overnight and the resulting solid was washed with toluene (2× 30 mL) and with Et$_2$O (2× 30 mL). Finally, the solids were dried for 4 h at r.t. in vacuo.

2.3. Catalytic test

2.3.1. Homogeneous systems

A flame dried 250 mL two-necked flask was fitted with a dropping funnel, flushed with nitrogen and charged with 2 g of activated, powdered 4 Å molecular sieves, 0.2 g (0.16 mmol) of **1** and 100 mL of dry CH_2Cl_2. After the mixture was cooled to −20 °C, 0.6 mL of a 5.5 M solution of t-BuOOH in nonane (3.2 mmol) was added. The mixture was allowed to stir at −20 °C for 1 h and then 0.4 mL of a 4.08 M solution of freshly distilled (E)-3-phenyl-2-propenol (cinnamyl alcohol) (1.61 mmol) diluted in 20 mL of CH_2Cl_2 added drop wise over 1 h. The resulting homogeneous solution was stirred 12 h at −20 °C. After this period the reaction mixture was quenched with 0.18 mL of a 10% aqueous solution of sodium hydroxide saturated with sodium chloride. The cold bath was removed and the mixture was allowed to stir for 10 additional minutes. Finally the organic layer was dried over anhydrous $MgSO_4$ and filtered through a celite bed, washing with Et_2O. The volatiles were then removed in vacuum obtaining a yellow oil (0.12 g, yield 50%, 24% ee). ^1H NMR (400 MHz, $CDCl_3$, 25 °C): $\delta = 2.15$ (br s, 1H, –OH), 3.22–3.25 (m, 1H, –CH-CH_2), 3.81 (dd, 1H, –CH_2), 3.94 (d, 1H, Ph-CH), 4.06 (dd, 1H, –CH_2), 7.2–7.4 (m, 5H, C_6H_5). The yields and enantiomeric excess values of the so obtained epoxy alcohols were determined by HPLC with a Chiralpak AD-H column from VWR International Eurolab [18].

2.3.2. Heterogeneous systems

A flame dried 250 mL two-necked flask was fitted with a dropping funnel, flushed with nitrogen and charged with 2 g of activated, powdered 4 Å molecular sieves, 0.5 g of catalyst Ti1-SBA-15-SiMe$_3$ and 50 mL of dry CH_2Cl_2. The mixture was cooled to −20 °C and tBuOOH in nonane was added. The mixture was allowed to stir at −20 °C for 1 h and then freshly distilled (E)-3-phenyl-2-propenol (cinnamyl alcohol) in CH_2Cl_2 (0.1 M), added drop wise over 1 h. The resulting mixture was stirred 12 h to −20 °C. The solid was recovered from the solution by filtration and washed several times with Et_2O. The volatiles were removed in vacuo to get a yellow oil (yield 45%, 23% ee). The solid was then treated with 2 equiv. of isopropanol in order to remove any organic species remaining adsorbed and then was tested again under similar experimental conditions.

2.4. Characterization

X-ray diffraction (XRD) patterns of the silicas were obtained on a Phillips Diffractometer model PW3040/00 X'Pert MPD/MRD at 45 kV and 40 mA, using Cu Kα radiation ($\lambda = 1.5418$ Å). N_2 gas adsorption–desorption isotherms were obtained using a Micromeritics TriStar 3000 analyzer, and pore size distributions were calculated using the Barret–Joyner–Halenda (BJH) model on the adsorption branch. Infrared spectra were recorded on a Nicolet-550 FT-IR spectrophotometer in the region 4000–400 cm^{-1} as Nujol mulls between polyethylene pellets and KBr disks. ^1H and $^{13}C\{^1H\}$ NMR spectra were recorded on Varian FT-300 and Varian FT-400 spectrometers and chemical shifts were measured relative

to residual ^1H and ^{13}C resonances in the deuterated solvents Proton-decoupled ^{29}Si MAS NMR spectra were recorded on a Varian-Infinity Plus 400 MHz Spectrometer operating at 79.44 MHz proton frequency (4 μs 90° pulse, 1024 transients, spinning speed of 5 MHz). Cross polarization ^{13}C CP/MAS NMR spectra were recorded on a Varian-Infinity Plus 400 MHz Spectrometer operating at 100.52 MHz proton frequency (4 μs 90° pulse, 4000 transients, spinning speed of 6 MHz, contact time 3 ms, pulse delay 1.5 s). Elemental analysis (%C and %N) was performed by the Investigation Service of the Universidad de Alcalá de Henares de Madrid (Spain) using a CHNS analyser LECO-932 model. The thermal stabilities of the modified mesoporous silicas were studied using a Setsys 18 A (Setaram) thermogravimetric analyzer. The DRUV–vis spectroscopic measurements were carried out on a Varian Cary-500 spectrophotometer equipped with an integrating sphere and PTFE (polytetrafluoroethylene) as reference, with $d = 1$ g/cm^3 and thickness of 6 mm. The titanium content was determined by ICP-atomic emission spectroscopy (ICP-AES) using a Varian Vista AX model. The samples (0.1 g) were dissolved in aqueous hydrofluoric and sulphuric acid. After dissolution, the sample was heated to evaporated water and hydrofluoric acid and the sample was transferred into 250 mL calibrated flask and diluted with water. Standard solution of Ti (1000 μg/mL in water) was used for the calibration of the equipment. HPLC analyses were performed on a Varian chromatographic system containing a 210/215 ProStar pump, a manual injection valve Rheodyne model 7752i equipped with a 20 μL sample loop, a 320 ProStar UV–vis detector and a personal computer-based data acquisition system Star Chromatography Workstation version 5. The chromatographic separations were performed, using a Chiralpak AD-H [amylose tris(3,5-dimethylphenylcarbamate) coated on silicagel, 250 mm × 4.6 mm i.d.; 10 μm particle diameter] column at ambient temperature.

3. Results and discussion

3.1. Preparation and characterization of monodentate titanium silsesquioxane complexes bearing menthoxo units

Reaction of silsesquioxane (c-C_5H_9)$_7$Si$_8$O$_{12}$(OH) with titanium(IV) alkoxo complex [{Ti(OiPr)$_2$(OMent)}$_2$] (**1**) previously reported by our group [19] occurs with protonolysis in THF solution, affording after CH_2Cl_2 recrystallization a white solid with the empirical formula [Ti(OiPr)$_2$(OMent){(c-C_5H_9)$_7$Si$_8$O$_{13}$}] {OMent = (1R,2S,5R)-(−)-menthoxo (**2**)} on the basis of elemental analysis and solution NMR data. The ^1H NMR spectrum of **2** in $CDCl_3$ contains the resonances attributed to the menthoxo ligand, as significative signal the multiplet assigned to CHO proton of menthoxo unit show a downfield shifted compared with that in free menthol ($\Delta\delta = \sim 0.5$) because their coordination to titanium and does not modified significantly their chemical shift respect to that of the parent titanium complex [{Ti(OiPr)$_2$(OMent)]$_2$}] due to the new (RO)Ti–O–Si bond formed. For correlation purposes and to study the way of introducing metallic catalysts we prepared

compound [Ti(OMent)$_3$(c-C$_5$H$_9$)$_7$Si$_8$O$_{13}$] (**4**), the protonolysis of (c-C$_5$H$_9$)$_7$Si$_8$O$_{12}$(OH) with the homoleptic tetrahedral titanium alkoxo complex [Ti(OMent)$_4$] (**3**) affords the expected (silsesquioxane)titaniumtrialkoxo in good yield, where titanium is incorporated via spatially oriented siloxy bond (Ti–O–Si) and surrounded by sterically demanding chiral groups. However, in the preparation of **4** the high boiling menthol produced could not be evacuated at 110 °C, 0.5 Torr, such a high temperature might promote decomposition, so this method turned out to be not effective for the preparation of pure [Ti(OMent)$_3${(c-C$_5$H$_9$)$_7$Si$_8$O$_{13}$}] (**4**) as can be observed on the basis of elemental analysis.

^{13}C and ^{29}Si NMR spectra of complexes **2** and **4** show a similar pattern of signals for the silsesquioxane unit than those reported by Duchateau for complexes [TiCl$_3${(c-C$_5$H$_9$)$_7$Si$_8$O$_{13}$}] [20] and [TiCp″(CH$_2$Ph)$_2${(c-C$_5$H$_9$)$_7$Si$_8$O$_{13}$}] (Cp″ = C$_5$H$_3$(SiMe$_3$)$_2$) [21]. ^{29}Si NMR spectra are particularly informative, the observation in each case of three resonances for the silsesquioxane Si atoms in 4:3:1 ratio. The cyclopentyl substituted silicon atoms show two resonances in a 3:4 ratio (**2**, −65.82, −67.04; **4** −66.37; −66.72), three of the seven silicon atoms, probably the closest to the metal are clearly distinct from the other four. Finally, the resonances of the silicon atoms surrounded by four oxygen atoms have characteristic chemical shifts of −113.48 (**2**) and −110.86 (**4**), respectively.
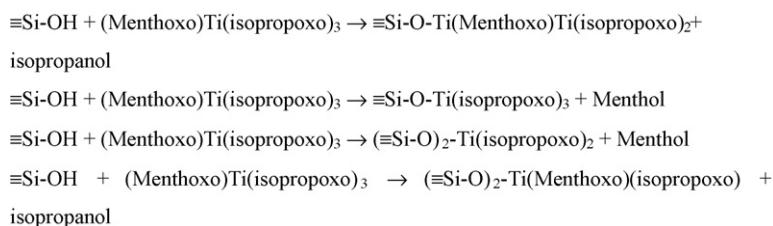
To gain insight into the chemistry of the grafting process, the reactions of [{Ti(O*i*Pr)$_2$(OMent)}$_2$] and [Ti(OMent)$_4$] with the monodentade (c-C$_5$H$_9$)$_7$Si$_8$O$_{12}$(OH) were monitored by ^{1}H NMR spectroscopy. In principle, the reaction of a surface bound –OH group or the silanol group of the silsesquioxane used in this study as model with the precursors should result in elimination of *i*PrOH and/or MentOH for complex **1** and MentOH for complex **2**. The products identified from the reaction in deuterated toluene after heating at 100 °C of complex **1** with the appropriate amount of the soluble silsesquioxane were both *i*PrOH and MentOH with an integral ratio 5:1, this suggests that the Ti–O*i*Pr bonds are more readily cleaved than Ti–OMent bond. Precursor **2** binds to the silica surface via Si–O–Ti–OMent linkages as expected.

3.2. Grafting procedures

Some problems must be take in account in the preparation of single site active catalyst by immobilization of titanium complexes **1** and **2** on hydrophobic silica based material were the intrinsic reactivity of the silanol groups, whose relatively low pK_a, make them incompatible with many of the reactions for

which metallic catalysts are used. Also the surface of silica-based materials is very hydrophilic, water can be absorbed through hydrogen bonds and liberated easily, and two adjacent silanol groups can for a Si–O–Si bridge expelling a molecule of water. This demonstrates the necessity to protect the Si–OH groups which can be done in several ways. Silylating reagents such as chlorosilanes, alkoxysilanes and sylilamines have found widespread applications and their reaction with surface silanol functionalities has been reported in detail [22]. A SBA-15 silica support was pretreated with chlorotrimethylsilane in order to convert –OH groups on the surface into –OSiMe$_3$, the silylation reaction was carried out by adding 10 mL of the chlorotrimethylsilane reagent diluted in toluene to 2 g of dehydrated SBA-15 suspended in 20 mL of toluene in the presence of the stoichiometric amount of triethylamine as additive. After stirring the reaction mixture at room temperature overnight the silylated material was washed twice with toluene, twice with THF and dried under vacuum for at least 5 h at 25 °C. The surface coverage 1.27 SiMe$_3$/nm^2 was calculated in bases of CHN elemental analysis [23] of the silylated samples by the following formula $\alpha(SiMe_3) = \delta(SiMe_3)N_A a_s^{-1} \times 10^{-18}$ (number of silyl groups per nm^2) being $\delta(SiMe_3) = \%C(100n_C M_C)^{-1}$ [mol/g] = concentration of surface silyl groups, %C = 7.99 wt% carbon referred to the parent SBA-15 silica; N_A = Avogadro constant $(6.022 \times 10^{23} \text{ mol}^{-1})$; a_s = specific BET surface area of dehydrated, non-modified SBA-15 (599 m^2/g); n_C = number of carbon atoms per silyl group (Si(CH$_3$)$_3$ 3); M_C = atomic weight of carbon (12.011 g/mol).

The titanium alkoxo complexes **1** and **2** have been tested as molecular precursors for the controlled synthesis of well-dispersed catalytic single sites. Derivatives **1** and **2** were grafted onto the silica support by stirring a suspension of the silylated support in a toluene solution of the precursor for 24 h under refluxing conditions. In this way Ti1-SBA-15-SiMe$_3$ and Ti2-SBA-15-SiMe$_3$ were obtained. Elemental analysis might be expected to give interesting information about Ti1-SBA-15-SiMe$_3$ and Ti2-SBA-15-SiMe$_3$ but since the Me$_3$SiO– groups and alkoxo ligands all contribute to the carbon content, this is no option. However, we determined the titanium content by inductively coupled plasma emission spectroscopy. The two samples studied here possessed titanium loading values of 0.91 and 0.20 mmol/g in agreement with the values obtained by Tilley et al. by using [(O*t*Bu)$_2$Ti{μ-O$_2$Si[OSi(O*t*Bu)$_3$]$_2$}]$_2$ [24] Ti[OSi(O*t*Bu)$_3$]$_4$, [(O*i*Pr)Ti[OSi(O*t*Bu)$_3$]$_3$, and [(O*t*Bu)$_3$Ti[OSi(O*t*Bu)]$_3$ [25] as precursors. The average pore diameter for the SBA-15 sample used in this study (57.9 Å) is much larger than the molecular
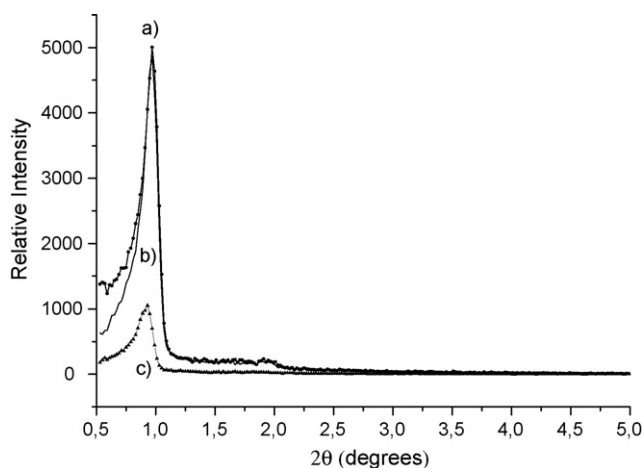
≡Si-OH + (Menthoxo)Ti(isopropoxo)$_3$ → ≡Si-O-Ti(Menthoxo)Ti(isopropoxo)$_2$+

isopropanol

≡Si-OH + (Menthoxo)Ti(isopropoxo)$_3$ → ≡Si-O-Ti(isopropoxo)$_3$ + Menthol

≡Si-OH + (Menthoxo)Ti(isopropoxo)$_3$ → (≡Si-O)$_2$-Ti(isopropoxo)$_2$ + Menthol

≡Si-OH + (Menthoxo)Ti(isopropoxo)$_3$ → (≡Si-O)$_2$-Ti(Menthoxo)(isopropoxo) +

isopropanol

Scheme 2.

Fig. 1. XRD patterns of (a) SBA-15, (b) Ti1-SBA-15-SiMe$_3$ and (b) Ti1-SBA-15-SiMe$_3$.

diameter of **1** and **2**. The titanium loading on SBA-15 after silylation obtained suggests the shrouding effect of the bulky alkoxo groups surrounding the titanium centre of these precursors. Indeed the less bulky precursor **1** can be supported onto the SBA-15 with much higher Ti loading, in addition the least sterically hindered precursor seems to be more reactive toward the protected silica support.

Solution ^{1}H NMR spectroscopy was used to monitor the grafting chemistry of **1** and **2** onto the silica surface. The reaction of unprotected surface Si–OH groups with a solution of a large excess of **1** should result in the elimination of isopropanol or menthol. The elimination products were indeed identified to be both *i*PrOH and MentOH with an integral ratio 3:1 after 48 h reaction in toluene at 100 °C. This result is in agreement with the formation of mono siloxy species bearing preferentially a chiral moiety, though bis(siloxy) titanium species cannot be excluded (Scheme 2).

3.3. Characterization of the samples

The XRD patterns for mesoporous silicas are shown in Fig. 1. Unmodified SBA-15 displayed a well-resolved pattern at low 2θ values with a very sharp (1 0 0) diffraction peak at 0.99° and an additional high order peak (1 1 0) at 1.96°. This system can be indexed as a hexagonal lattice with *d*-spacing values of 89.46 and 45.06 Å, respectively. A unit cell parameter, a_0, of 103.30 Å was obtained using the following equation $a_0 = 2d_{1 0 0}/\sqrt{3}$ [17]. The slightly decrease in the intensity of the (1 0 0) XRD diffraction peak at 0.99° in Ti1-SBA-15-SiMe$_3$ and the significant further loss in Ti2-SBA-15-SiMe$_3$ observed after immobilization of the titanium complexes provides further evidence that

grafting mainly occurs inside the mesopore channels, since the attachment of organic functional groups in the mesopore channels tends to reduce the scattering power of the mesoporous silicate wall. The XRD pattern of the functionalized SBA-15 also suggests that the structural order of the synthesized material is maintained after functionalization.

The textural properties such as specific surface area (S_{BET} (m^2 g^{-1})) and pore volume (cm^3 g^{-1}) of the support were followed throughout the different modification processes. For the parent SBA-15 system and functionalized materials Ti1-SBA-15-SiMe$_3$ and Ti2-SBA-15-SiMe$_3$ the isotherms are type IV according to the IUPAC classification and have an H1 hysteresis loop that is representative of mesoporous cylindrical or rod-like pores (Fig. 2). The volume adsorbed for all isotherms increased sharply at a relative pressure (P/P_0) of 0.4, which represents capillary condensation of nitrogen within the uniform mesoporous structure. The inflection position shifted slightly to lower relative pressures and the volume of nitrogen adsorbed decrease upon silylation and titanium grafting, which is indicative of a reduction in the pore size because of the anchoring of titanium complexes inside the channels. The physical parameters of the nitrogen isotherms, such the Brunauer–Emmett–Teller surface area (S_{BET}), total pore volume and BJH average pore diameter, for mesoporous silicas are shown in Table 1. The synthesized material possessed high S_{BET} (599 m^2/g), a pore volume of 0.61 cm^3/g and a BJH pore diameter of 57.9 Å, these values are typical of surfactant-assembled mesostructures. The wall thickness for SBA-15 (45.39 Å) was calculated as ($2d_{1 0 0}/\sqrt{3}$-BJH pore diameter). After silylation and Ti grafting, a decrease in the S_{BET}, pore volume and average BJH pore diameter were observed (Table 1), changes that can be interpreted as being due to the presence of organotitanium molecules on the surface partially blocking the adsorption of nitrogen molecules. The narrow pore size distributions found for Ti1-SBA-15-SiMe$_3$ and Ti2-SBA-15-SiMe$_3$ (centred at 54.4 and 54.5 Å) provide evidence for its uniform framework mesoporosity (Fig. 3).

The IR patterns of mesoporous silicas between 4000 and 400 cm^{-1} are shown in Fig. 3. The main features of the SBA-15 spectra include a large broad band between 3400 and 3200 cm^{-1}, which is attributed to O–H stretching of the surface silanol groups and the remaining adsorbed water molecules. The siloxane (–Si–O–Si–) band appears as a broad strong peak centred at 1100 cm^{-1}. The band due to Si–O bond stretching of the silanol groups was observed at 900 cm^{-1}. The adsorption band at 1630 cm^{-1} is due to deformation vibrations of adsorbed water molecules [26]. The Ti1-SBA-15-SiMe$_3$ and the Ti2-SBA-15-SiMe$_3$ systems showed characteristic bands for aliphatic C–H stretching vibrations due to OSiMe$_3$ and alkoxo groups. The bands typical of

Table 1
Physical parameters of mesoporous silicas measured by N$_2$ adsorption–desorption isotherms

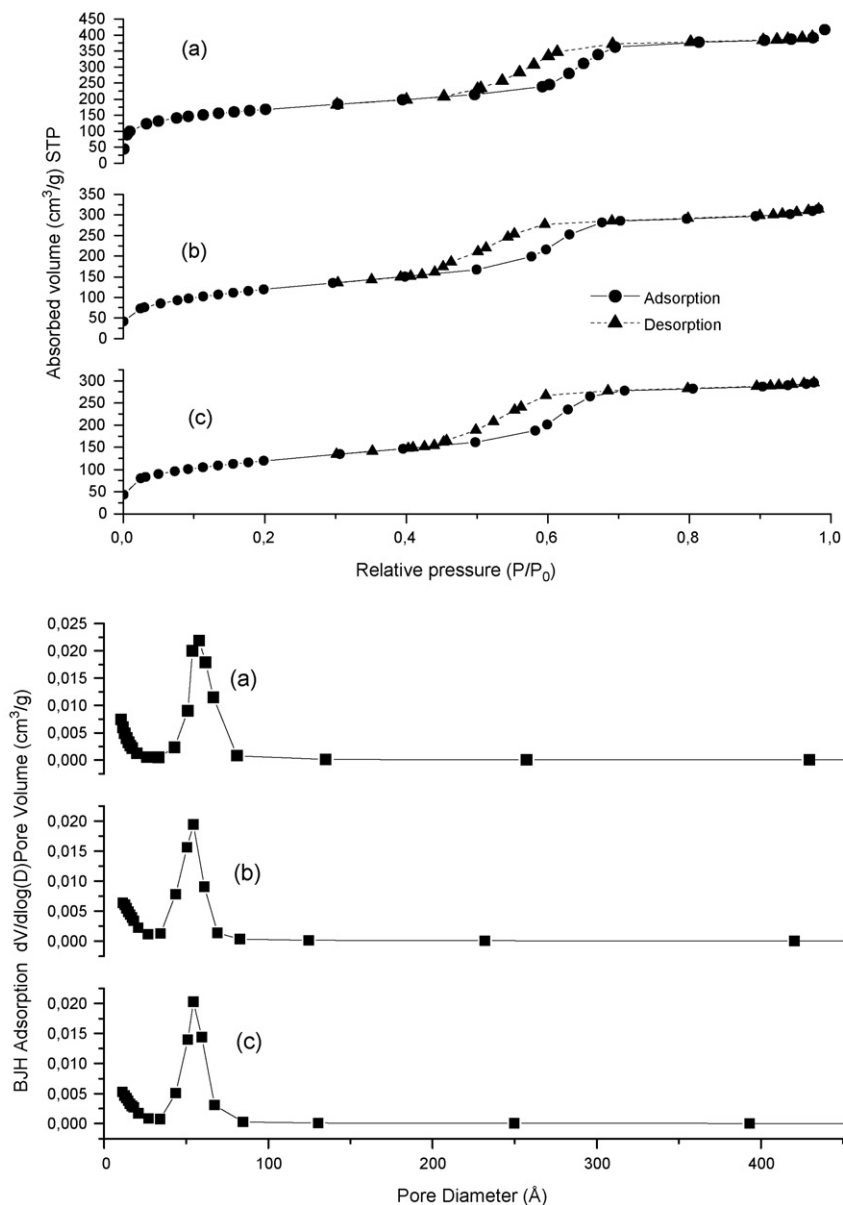| Material	S_{BET} (m^2/g)	Pore diameter[a] (Å)	Pore volume (cm^3/g)	Wall thickness (Å)
SBA-15	599	57.9	0.61	45.39
Ti1-SBA-15-SiMe$_3$	433	50.5	0.48	53.29
Ti2-SBA-15-SiMe$_3$	434	54.4	0.45	55.37

[a] BJH: Barret, Joynet and Halenda.

Fig. 2. Nitrogen adsorption–desorption isotherms and pore size distribution of (a) SBA-15, (b) Ti1-SBA-15-SiMe$_3$ and (c) Ti2-SBA-15-SiMe$_3$.

menthoxo groups appear at 2960 cm^{-1} (ν_{as}(CH$_3$)), 2929 cm^{-1} (ν_{as}(CH$_2$)), 2877 cm^{-1} (ν_{s}(CH$_3$)), 2852 cm^{-1} (ν_{s}(CH$_2$)), 1457 and 1455 cm^{-1} (δ_{a}(CH$_2$), δ_{a}(CH$_3$)), and 1388 and 1369 cm^{-1} δ_{s}(CH$_3$), the two last bands are characteristics of isopropyl groups. The decrease of the broad band between 3400 and 3200 cm^{-1} explained as the signals of the OH stretching vibration of the silanol groups on the surface of the SBA-15, shows the capping procedure using trimethylsilyl groups to be satisfactory for the use in reaction involving organotitanium reagents. However, this peak assignment was later at around 2960, 849 and 755 cm^{-1}. The absorption peak at 950–970 cm^{-1} is assigned to Ti–O–Si bonds.

The ^{29}Si MAS NMR spectra in the solid state for parent SBA-15 and functionalized silica (Ti2-SBA-15-SiMe$_3$ and Ti1-SBA-15-SiMe$_3$) confirm the covalent bond formed between the silylating agent Me$_3$SiCl and the silanol groups dispersed on the SBA-15 surface (see Fig. 4). Unmodified silica (SBA-15, Fig. 4a) shows two main peaks at -110 and -98 ppm assigned to Q^4 framework silica sites ((SiO)$_4$*Si*) and Q^3 silanol sites ((SiO)$_3$*Si*OH), respectively. A weak resonance is also present at about -92 ppm corresponding to the Q^2 species ((SiO)$_2$*Si*(OH)$_2$), Q^4 is clearly the dominant peak in both spectra because it is the most abundant site. The spectra of the functionalized silica show a marked decrease in the intensity of the Q^3 signal, which verified the anchoring of the functional groups to Si–OH. In addition, the choice of these particular protecting groups allows an easy determination of the trimethylsilyl groups by ^{29}Si NMR; the new peak of the silylating agent, an M site (Me$_3$*Si*O–), is seen at 12 ppm.

Important features related to the immobilization of titanium complexes **1** and **2** on the inorganic structure can be obtained from ^{13}C MAS NMR spectra in the solid state, as shown in
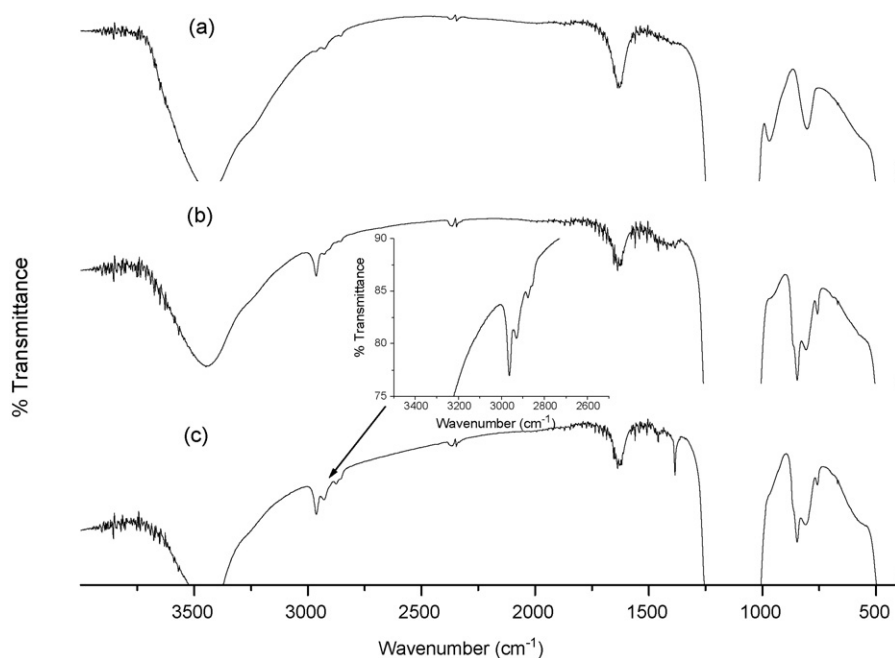
Fig. 3. FT-IR of (a) SBA-15, (b) Ti1-SBA-15-SiMe$_3$ and (c) Ti2-SBA-15-SiMe$_3$.

Fig. 5 for Ti2-SBA-15-SiMe$_3$. In this figure we can observe at δ -0.1 ppm the signal due to the trimethylsilyl carbon atoms of the silylating agent $(CH_3)_3SiO$ and the signals of the 10 carbons of the menthoxo group (C1–C10). Their respective chemical shifts are listed in Table 2 , Comparing the spectra of compound **2** and the spectrum of the grafted specie Ti2-SBA-15-SiMe$_3$ most of the peaks in the solid phase spectrum have a corresponding signal in the liquid phase spectrum of the reference compound.

Diffuse reflectance UV–vis spectroscopy (DRUV–vis) is a useful corroborative tool to suggest the presence of four-coordinate Ti(IV) sites. The DRUV–vis spectrum of Ti1-SBA-15-SiMe$_3$ as showed in Fig. 6a (taken under ambient air conditions) exhibits a strong absorption at $\lambda_{max} = 230$ nm for
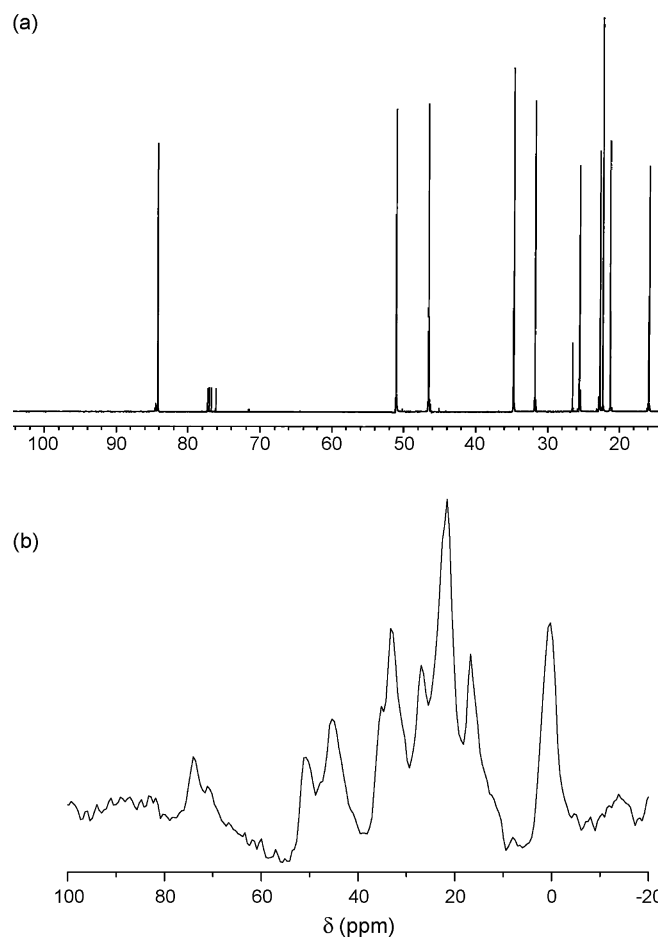

Fig. 4. ^{29}Si MAS NMR spectra of (a) SBA-15, (b) Ti1-SBA-15-SiMe$_3$ and (c) Ti2-SBA-15-SiMe$_3$.

Fig. 5. (a) ^{13}C NMR spectra of [Ti(OMent)$_4$] and (b) ^{13}C MAS-NMR spectra of Ti2-SBA-15-SiMe$_3$.
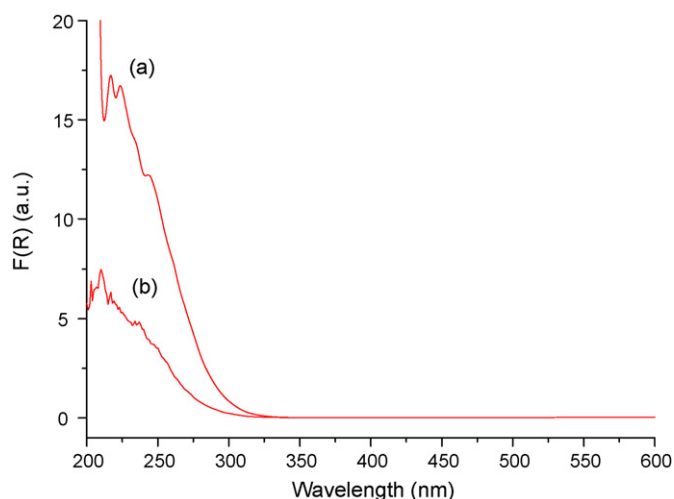
Fig. 6. Diffuse reflectance UV–vis spectra of (a) Ti1-SBA-15-SiMe$_3$ and (b) Ti2-SBA-15-SiMe$_3$ in ambient conditions.

Table 2
^{13}C NMR chemical shifts in ppm for [Ti(OMent)$_4$] and Ti2-SBA-15-SiMe$_3$

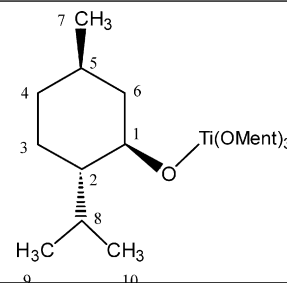|	[Ti(OMent)$_4$]	Ti2-SBA-15-SiMe$_3$
C1	84.1	73.6
C2	51.0	50.3
C3	22.7	21.4 (C$_9$ + C$_7$ + C$_3$)
C4	34.6	32.6 (C$_4$ + C$_5$)
C5	31.7	32.6 (C$_4$ + C$_5$)
C6	46.5	45.0
C7	22.3	21.4 (C$_9$ + C$_7$ + C$_3$)
C8	25.5	26.2
C9	21.2	21.4 (C$_9$ + C$_7$ + C$_3$)
C10	15.8	16.2

the oxygen to Ti(IV) charge transfer band (LMCT). Similarly, the DRUV–vis spectrum of Ti2-SBA-15-SiMe$_3$ as showed in Fig. 6b contains an absorption at $\lambda_{max} = 220$ nm. Absorption maxima in the range of 210–240 nm are attributed to a LMCT for true four-coordinate Ti(IV). A broad shoulder at 270–280 is observed, these absorption bands in the region of 250–280 nm have been assigned to centres with water coordinated to isolated Ti(IV) sites. Bulk anatase displays an absorption maximum at ca. 330 nm. Thus, DRUV–vis spectroscopy indicates that these materials (under ambient air atmosphere) possess titanium centres that may be described as four coordinate Ti(OSi)(OR)$_3$ or Ti(OSi)$_2$(OR)$_2$ species, possibly with some degree of water coordination [24].

In thermogravimetric experiments we found Ti1-SBA-15-SiMe$_3$ to be stable up to at least 185 °C (less than 0.3% weight loss). The profiles indicate that the unmodified silica (Fig. 7a) shows a small loss in mass (7.2%) in a first step between room temperature and 150 °C due to the loss of physically adsorbed water (endothermic process). A second decrease in mass of 0.1% (between 600 and 800 °C) is attributed to the increase in the number of siloxane bridges (Si–O–Si) due to isolated silanol condensation (exothermic process). The TGA curves (Fig. 7b and c) of the modified material Ti1-SBA-15-SiMe$_3$ and Ti2-SBA-15-SiMe$_3$ show that a degradation process occurs in two steps in the fist step between 185 and 300 °C the weight loss is about 1.18%—this is due to the break down of titanium complexes anchored on the SBA-15 surface (exothermic process). Between 300 and 545 °C the weight loss is about 2.11% and it is attributed to the break down of silylating agent Me$_3$SiO-anchored on the SBA-15 surface, the expected small degree of silanol condensation is hidden by the loss of organic matter in the second decomposition step. The thermal stability of these samples is also in agreement with previous results given in the literature for other functionalized mesoporous silicas [27].
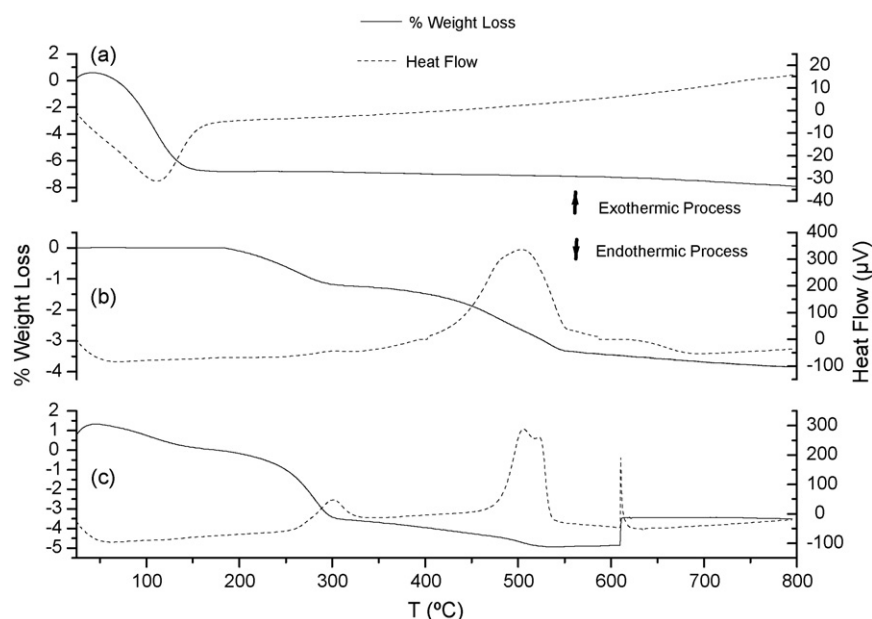

Fig. 7. Thermogravimetric curves and heat flow of (a) SBA-15, (b) Ti1-SBA-15-SiMe$_3$ and (c) Ti2-SBA-15-SiMe$_3$.

Table 3
Comparison of the ee, yield and absolute configuration obtained in asymmetric epoxidation of cinnamyl alcohol

Catalyst	Catalyst/substrate ratio (mol/mol)				Absolute configuration
	1/2		1/10		
	Yield (%)	ee (%)	Yield (%)	ee (%)	
Ti1-SBA-15-SiMe$_3$	60	27	45	23	2S,3S
Ti2-SBA-15-SiMe$_3$	12	8	16	3	2S,3S
Ti(O^{i}Pr)$_2$(OMent)(OSilox)	58	15	62	13	2S,3S
Ti(O^{i}Pr)$_2$(OMent)$_2$	13	58	50	24	2R,3R

3.4. Catalytic allylic alcohol epoxidation

In this work we reasoned that masking a part of surface–OH groups with trimethylsilyl groups would improve the activity of the catalysts. The modified materials Ti1-SBA-15-SiMe$_3$ and Ti2-SBA-15-SiMe$_3$ were tested as catalysts for the liquid phase epoxidation of cinnamyl alcohol with tBuOOH at −20 °C. Allylic alcohol conversion in the absence of catalyst or in the presence of the parent SBA-15 was negligible under similar experimental conditions. For comparison complexes **1** and **2** were also tested as homogeneous pre-catalyst for the same reaction obtaining in both cases the (2R,3R)-epoxide as the preferred enantiomer. With complex **1**, described as a dinuclear complex in which the two metal atoms are joined through an isopropoxo bridge adopting an edge-bridged bis(trigonal bipyramidal) coordination environment, a yield of 50% and 24% enantiomeric excess was obtained, as can be seen in Table 3. The sterically demanding complex **2** with the titanium atom tetrahedrally coordinated, led to an important decrease in both values.

The titanium silsesquioxane complex **3** catalyses the epoxidation of alkenes under similar conditions obtaining better yields but lower enantiomeric excess. An essential feature of several of the proposed mechanisms of alkene epoxidation by titanium silsesquioxane derivatives involves hydrolysis of a titanium siloxy function in a four-coordinate active site, such a hydrolysis step would lead to rapid degeneration of the complex **3** since the titanium siloxy units (Ti–O–Si) result here from functionalization of isolated silanol groups, the silsesquioxane being a bifunctional monodentate ligand. This would therefore imply that the active catalyst responsible of the epoxidation would be homogeneous non-siloxy species similar to those generated by complex **2**. Nevertheless, the experimental results show that the (2S,3S)-epoxide is obtained as the preferred enantiomer the same as the enantiomer obtained by the heterogeneous systems under study Ti1-SBA-15-SiMe$_3$ and Ti2-SBA-15-SiMe$_3$. It should be noted that the catalyst Ti2-SBA-15-SiMe$_3$ prepared with complex **2** as a reference showed much less catalytic activity than catalyst Ti1-SBA-15-SiMe$_3$, probably due to the presence of more steric hindrance arisen from larger menthoxo groups with respect to smaller isopropoxo groups present in Ti1-SBA-15-SiMe$_3$. The reactivity of these catalysts is dependent upon the nature of the ligands surrounded the titanium atom. The chirality is provided by (−)-menthoxo groups bonded to titanium. Indeed the menthoxo fragment is chiral and presents an important steric hindrance which allows it to interact strongly with

Table 4
Recycle performance of Ti1-SBA-15-SiMe$_3$ catalyst

No.	Catalyst/substrate ratio (mol/mol) [1/10]	
	Yield (%)	ee (%)
1	45	23
2	39	18
3	22	11

substrate molecules at the pore channel of the mesoporous solid (Table 4).

The stabilities of the modified material Ti1-SBA-15-SiMe$_3$ was studied by recycling the recovered solid twice. Before each reuse the solid was separated from the reaction solution, thoroughly washed with dichloromethane and the appropriate amount of isopropanol and dried at room temperature. We have found that in successive runs both, the activity and the enantiomeric excess of the reaction have decreased. This trend can be interpreted by considering two points. Firstly, by leaching processes and secondly by loss of the chiral moieties bonded to titanium.

4. Conclusions

Mesoporous materials offer an openly accessible pore structure in all possible solvents and in a wide temperature and pressure range. Post-synthetic modification of structurally highly order SBA-15 offers an alternative route, here we report the preparation of chiral titanium centres on a mesoporous protected silica surface in relatively high loading, this method eliminates the common problems that limit the titanium well known coordination sphere because silanol groups reactivity, although side reactions leading to non-chiral species or involving two surface silanol groups, limit the selectivity of the grafting reaction of organotitanium complexes. The results obtained in the catalytic epoxidation of cinnamyl alcohol, show similar enantioselectiviy for heterogeneous systems and silsesquioxane complex **3**, meanwhile the pre-catalyst **1** and **2** under homogeneous conditions led to the complementary enantiomer, suggesting that the characteristics of the chiral titanium unit may play an important role in the control of enantioselectivity, i.e., the steric repulsion between the metal-binding site and substrate.

Acknowledgements

References

[1] (a) T. Uozumi, T. Toneri, K. Soga, T. Shiono, Macromol. Rapid Commun. 18 (1997) 9;
(b) A.M. Uusitalo, T.T. Pakkanen, E.I. Iskola, J. Mol. Catal. A: Chem. 177 (2002) 179;
(c) J.H. Zimnoch dos Santos, P.P. Greco, F.C. Stedile, J. Dupont, J. Mol. Catal. A: Chem. 154 (2000) 103;
(d) N. Suzuki, J. Yu, N. Shioda, H. Asamib, T. Nakamura, T. Huhn, A. Fukuoka, M. Ichikawa, M. Saburi, Y. Wakatsuki, Appl. Catal. A 224 (2002) 63.

[2] H. Juvaste, T.T. Pakkanen, E.I. Iiskola, Organometallics 19 (2000) 4834.

[3] W.H. Zhang, J.L.B. Han, M. Li, J. Xiu, P. Ying, C. Li, Chem. Mater. 14 (2002) 3413.

[4] G. Calleja, R. Van Grieken, R. García, J.A. Melero, J. Iglesias, J. Mol. Catal. A: Chem. 182–183 (2002) 215.

[5] P. Ferreira, I.S. Gonçalves, F.E. Kühn, M. Pillinger, J. Rocha, A.M. Santos, A. Thursfield, Eur. J. Inorg. Chem. (2000) 551.

[6] (a) P. Iengo, G. Aprile, M. Di Serio, D. Gazzoli, E. Santacesaria, Appl. Catal. A: Gen. 178 (1999) 97;
(b) Z. Luan, E.M. Maes, P.A.W. Van der Heide, D. Zhao, R.S. Czernuszewicz, L. Kevan, Chem. Mater. 11 (1999) 3680.

[7] (a) M.C. Capel-Sánchez, J.M. Campos-Martín, J.L.G. Fierro, M.P. de Frutos, A. Padilla Polo, Chem. Commun. (2000) 855;
(b) I. Mandache, V.I. Parvulescu, A. Popescu, L. Parvulescu, M.D. Banciu, P. Amoros, D. Beltran, D. Trong On, S. Kaliaguine, Micropor. Mesopor. Mater. 81 (2005) 115;
(c) Z. Fu, D. Yin, Q. Xie, W. Zhao, A. Liu, D. Yin, Y. Xu, L. Zhang, J. Mol. Catal. A: Chem. 208 (2004) 159.

[8] R. Duchateau, Chem. Rev. 102 (2002) 3525.

[9] H.C.L. Abbenhuis, S. Krijnen, R.A. Van Santen, Chem. Commun. (1997) 331.

[10] T. Maschmeyer, M.C. Klunduk, C.M. Martin, D.S. Shephard, J. Meurig Thomas, B.F.G. Johnson, Chem. Commun. (1997) 1847.

[11] M. Crocker, R.H.M. Herold, A.G. Orpen, M.T.A. Overgaag, J. Chem. Soc., Dalton Trans. (1999) 3791.

[12] S. Krijnen, H.C.L. Abbenhuis, R.W.J.M. Hanssen, J.H.C. van Hooff, R.A. van Santen, Angew. Chem. Int. Ed. 3 (1998) 37.

[13] M.C. Klunduik, T. Maschmeyer, J.M. Thomas, B.F.G. Johnson, Chem. Eur. J. 5 (1999) 5.

[14] D. Meunier, A. Piechaczyk, A. Mallmann, J.M. Basset, Angew. Chem. Int. Ed. 23 (1999) 38.

[15] S. Xiang, Y. Zhang, Q. Xin, C. Li, Angew. Chem. Int. Ed. 5 (2002) 41.

[16] A. Heckel, D. Seebach, Chem. Eur. J. 8 (2002) 560.

[17] D. Zhao, Q. Huo, J. Feng, B.F. Chmelka, G.D. Stucky, J. Am. Chem. Soc. 120 (1998) 6024.

[18] S. Morante-Zarcero, Y. Pérez, I. del Hierro, M. Fajardo, I. Sierra, J. Chromatogr. A 1046 (2004) 61.

[19] Y. Pérez, I. del Hierro, M. Fajardo, A. Otero, J. Organomet. Chem. 679 (2003) 220.

[20] R. Duchateau, H.C.L. Abbenhuis, R.A. van Santen, A. Meetsma, S.K.H. Thiele, M.F.H. van Tol, Organometallics 17 (1998) 5663.

[21] R. Duchateau, H.C.L. Abbenhuis, R.A. van Santen, S.K.H. Thiele, M.F.H. van Tol, Organometallics 17 (1998) 5222.

[22] (a) L.H. Dubois, B.R. Zegarski, J. Am. Chem. Soc. 115 (1993) 1190;
(b) N. Suzuki, J. Yu, N. Shioda, H. Asami, T. Nakamura, T. Huhn, A. Fukuoka, M. Ichikawa, M. Saburi, Y. Wakatsuki, Appl. Catal. A: Gen. 224 (2002) 63.

[23] R. Anwander, I. Nagl, M. Widenmeyer, G. Engelhardt, O. Groeger, C. Palm, T. Ro1ser, J. Phys. Chem. B 104 (2000) 3532.

[24] R.L. Brutchey, B.V. Mork, D.J. Sirbuly, P. Yang, T.D. Tilley, J. Mol. Catal. A: Chem. 238 (2005) 1.

[25] J. Jarupatrakorn, D.T. Tilley, J. Am. Chem. Soc. 124 (2002) 8380.

[26] (a) E. Pretsch, T. Clero, J. Seibl, W. Simon, Tablas para la elucidación estructural de compuestos orgánicos por métodos espectroscópicos, Alhambra, Madrid, 1991D;
(b) P.G. Lampman, G. Kriz, Introduction to Spectroscopy, Harcourt College Publishers, USA, 2001.

[27] (a) B. Lee, Y. Kim, H. Lee, J. Yi, Micropor. Mesopor. Mater. 50 (2001) 77;
(b) D.J. Macquarrie, D.B. Jackson, J.E.G. Mdoe, H.J. Clark, New J. Chem. 23 (1999) 539;
(c) L. Bois, A. Bonhommé, A. Ribes, B. Pais, G. Raffin, F. Tessier, Colloids Surf. A: Physicochem. Eng. Asp. 221 (2003) 221.